

# Quantum-Dot Semiconductor Optical Amplifier: Performance and Application for Optical Logic gates

Ali Farmani<sup>1</sup>, Mohammad Hossein Sheikhi<sup>1</sup>

1- Department of Electrical and Computer Engineering, Shiraz University, Shiraz Iran.

Email: ali.farmani@shirazu.ac.ir (Corresponding author)

Received: August 2017

Revised: August 2017

Accepted: August 2017

## ABSTRACT:

We proposed a novel structure of ultrafast all optical Feynman logic gate based on the cross-phase modulation that is principle nonlinear effect in a quantum dot semiconductor optical amplifier assisted with a Mach-Zehnder interferometer at the wavelength of 1.55  $\mu\text{m}$ . To realize ultrafast mechanism, an active layer with a thickness of 1.7- $\mu\text{m}$ , and the confinement factor of 0.75 and 0.7 respectively for both  $\text{TE}_0$  and  $\text{TM}_0$  modes, are provided. By solving the rate equations, a gain difference up to 0.1 dB has been obtained. The proposed structure has the potential application in advanced optical devices such as optical memristors.

**KEYWORDS:** Semiconductor Optical Amplifier, Optical Logic gate, Cross-Phase Modulation, Mach-Zehnder Interferometer.

## 1. INTRODUCTION

In recent years, in advanced telecommunication systems, the rate of the data transmission has been considered. Up to now, all optical systems with high data transmission capability are highly desirable to support the all optical signal processing [1]. Logic gates are one of the key elements for ultrafast signal processing such as ultrafast advanced encryption and decryption [2], [3], arithmetic operations and complicated processing circuits (e.g., multiplier, shift registers, counter, and central processing unit). [4]- [8]. Typically, all optical logic gates using optical components which work base on the nonlinear effect of medium [9]. Hence, the optical logic gates are divided into two categories based on nonlinear mechanism including optical fiber logic gates and semiconductor optical amplifier (SOA) logic gates [10], [11]. However, the optical fiber has a weak nonlinearity, and high power pump needs to achieve reasonable switching efficiency. The SOA has a small size and electrically pumped, also SOA less expensive than optical fiber amplifier and can be integrated with an optical component such as a laser, modulator and multiplexer [12]. In the different methods, integrated Mach-Zehnder interferometer (MZI) based on SOA has been developed as a practical platform for logic gates due to its compact size [13], thermal stability and low power consumption. All optical Feynman gates as one of the quantum logic gates implemented with various nonlinearities in SOA including cross gain modulation (XGM), cross phase modulation (XPM) and four wave

mixing (FWM) which enable switching light to another wavelength [14-16].

In this paper, different from the previous works, to realize ultrafast logic mechanism, we first propose a quantum dot (QD) InAs/GaAs SOA, in which only  $\text{TE}_0$  and  $\text{TM}_0$  modes can propagate. We show that it is possible to obtain good polarization insensitivity (sensitivity < 0.1 dB) for proposed SOA. That is obtained by solving the rate equations. Then, by considering the XPM effect, we use the above-mentioned structure to realize of Feynman logic gates. Finally, based on the numerical results it is suggested that the structure is a good candidate for future optical logic gates.

The remainder of the paper is organized as follows. In Section 2 the principle of operation and structure of SOA is studied. Then we derive, analyze, and interpret results on the performance of the all optical Feynman logic gate. In Section 3 we provide the discussion of the proposed logic gate. Finally, in Section 4. We summarize the main findings of our work and simulation results.

## 2. THE SOA PRINCIPLE WORK

Owing to the significant effect of active layer thickness in SOA, by considering a suitable thickness for the active layer and also by choosing the lattice matching for the wavelength of the optical pumping, it allows harnessing the propagation of TE and TM in the semiconductor optical amplifier. Hence, the investigation of the thickness and wavelength

sensitivity of the SOA in quantum dot structure is a helpful method to characterize the thick behavior of SOAs. In Fig. 1 we illustrate the configuration of the proposed quantum dot SOA. We assign the direction of wave propagation as the z-axis and the index profile is independent of z as well. The electric field  $E(x,y,z)$  and magnetic field  $H(x,y,z)$  propagation along the z direction.

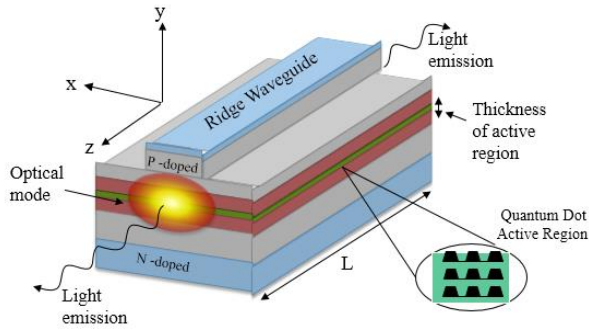


Fig. 1. The three dimensional schematic of the proposed QD-SOA.

As a next step, we have presented the band structure (BS) of the structure. The BS of the InAs/GaAs QD-SOA is shown in Fig. 2.

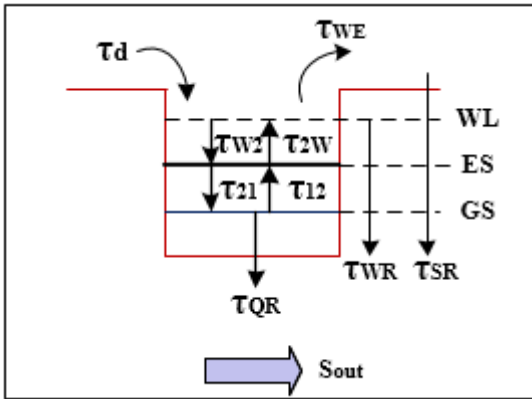


Fig. 2. Energy diagram Band of the proposed Quantum Dot Semiconductor Optical Amplifier structure.

In Fig. 2 we considered the spontaneous emission, the stimulated absorption, the stimulated emission and the non-radiative transitions. The input light is focused into SOA by considering a microscope objective lens with the focal length of 4.6mm (numerical aperture=0.65). Moreover, the proposed structure is InAs/GaAs QD-SOA with the length of a 10μm.

The active layer of the SOA was sandwiched between InAs layers (17 Å) with a bandgap wavelength of 0.9μm. Optical mode confinement factors for TE<sub>0</sub> and TM<sub>0</sub> modes are calculated by the conventional slab waveguide analysis using refractive indices of 3.53 and 3.37, for the active layer and the

cladding layer, respectively at the wavelength of 1.55μm, as shown in Fig. 3 and Fig. 4.

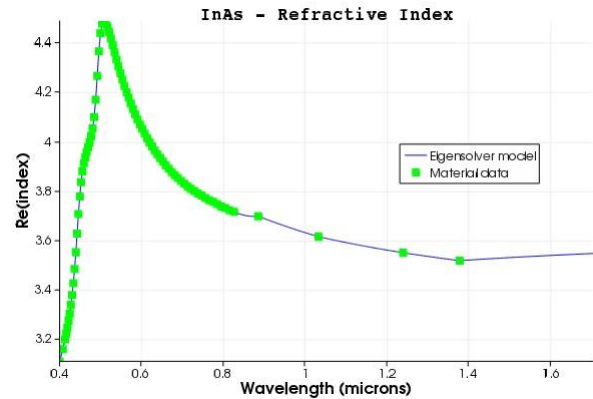


Fig. 3. The numerical calculation of the refractive index of InAs.

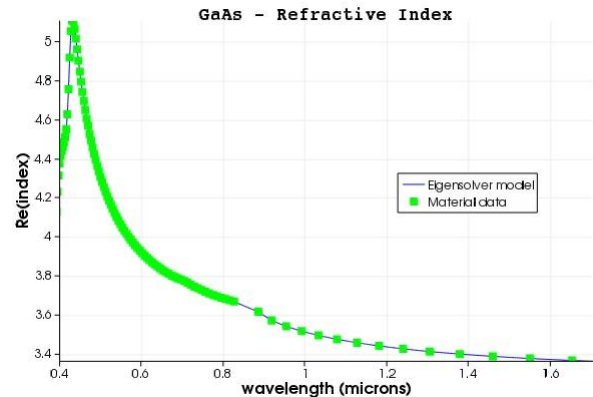


Fig. 4. The numerical calculation of the refractive index of GaAs.

To calculate gain and power we must solve the three-level rate equation for the electron transmission between the wetting layer (WL), excited state (ES), and ground state (GS) respectively, which are as follows [12]:

$$\frac{\partial N_w}{\partial t} = \frac{N_s L_s}{\tau_d L_w} + \frac{N_w h}{\tau_{2w}} - \frac{N_w(1-h)}{\tau_w} - \frac{N_w}{\tau_{WR}} - \nu_g \Gamma_{g_w} S \quad (1)$$

$$\frac{\partial (N_Q h)}{\partial t} = \frac{N_w(1-h)}{\tau_w} + \frac{N_Q(1-h)f}{\tau_{12}} - \frac{N_Q(1-f)h}{\tau_{21}} - \frac{hN_w}{\tau_{2w}} - \frac{hN_Q}{\tau_{2R}} - \nu_g \Gamma_{g_{ES}} S \quad (2)$$

$$\frac{\partial (N_Q f)}{\partial t} = \frac{N_Q(1-f)h}{\tau_{21}} - \frac{N_Q(1-h)f}{\tau_{12}} - \frac{N_Q}{\tau_{1R}} f^2 - \nu_g \Gamma_{g_{GS}} S - \nu_g \Gamma_{g_1} S(2f-1) \quad (3)$$

and the photon rate equation is

$$\frac{\partial S}{\partial t} = \nu_g \Gamma_{g_w} S + \nu_g \Gamma_{g_{ES}} S + \nu_g \Gamma_{g_{GS}} S - \frac{S}{\tau_{ph}} \quad (4)$$

where h is the electron occupation probability of the

ES,  $f$  is the electron occupation probability of the GS,  $\tau_{w2}$  is the electron relaxation time (ERT) from the WL to the ES,  $\tau_{2w}$  is the electron escape time (EET) from the ES to the WL,  $\tau_{wR}$  is the spontaneous radiative lifetime (SRL) in WL,  $\tau_{21}$  is the ERL from the ES to GS,  $\tau_{12}$  is the EET from the GS to the ES,  $\tau_{1R}$  and  $\tau_{2R}$  are the SRL in the QD GS and ES respectively.  $N_Q$  is the density of the QDs,  $N_w$  is the electron density in the WL and  $L_w$  is the effective thickness of the WL and  $\tau_{ph}$  is the cavity photon lifetime. The electromagnetic field profile is simulated using finite difference time domain (FDTD) method. The carrier density and photon density are calculated by solving the rate equations, as depicted in Fig. 5.

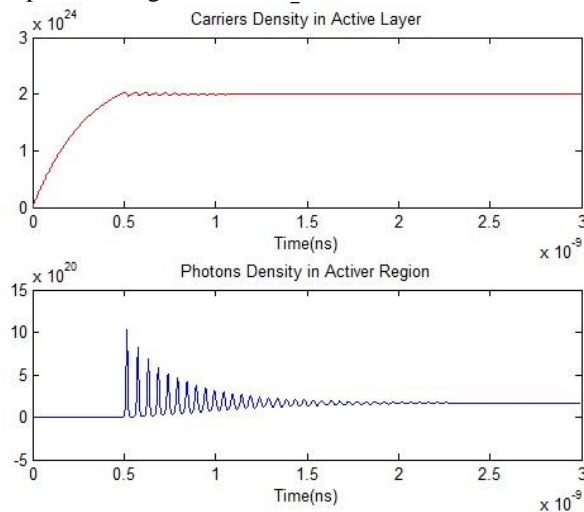


**Fig. 5.** Carrier density and photon density calculated from the rate equation.

Fig. 6a shows the numerical calculated far-field pattern (FFP) along the vertical and horizontal directions to the junction plane. The full-width at half-maximum (FWHM) of the FFPs was numerically calculated as  $30^\circ \times 30^\circ$ . Moreover, the calculated field profile is shown in Fig. 6b.

Table 1 provides the structural parameters of a QD-SOA for rate equation.

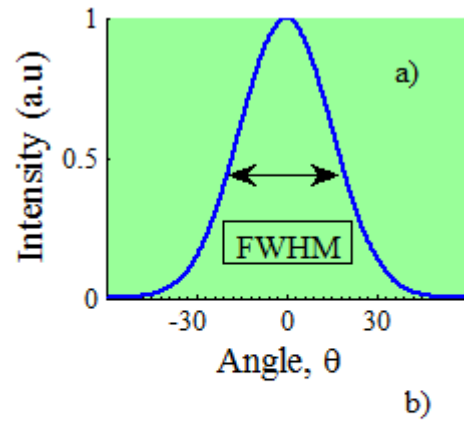


**Fig. 6.** a): the FWHM of the proposed structure, b): the field profile of the QD-SOA.

**Table 1.** Major structural parameters of a quantum dot semiconductor amplifier in rate equation approach.

Symbol	Definition	Value
$L$	Thickness of active layer	$1.7 \mu\text{m}$
$\Gamma$	Confinement factor	$0.7$
$\lambda$	Wavelength	$1.55 \mu\text{m}$
$\tau_{w2}$	ERT from WL $\rightarrow$ ES	$3 \text{ ps}$
$\tau_{2w}$	EET from ES $\rightarrow$ WL	$1 \text{ ns}$
$\tau_{1R}$	SRL in WL	$0. \text{ ns}$
$\tau_{21}$	ERL from ES $\rightarrow$ GS	$0.15 \text{ ps}$
$\tau_{12}$	EET from GS $\rightarrow$ ES	$1 \text{ ps}$
$N_Q$	Density of QDs	$2 \cdot 10^{24} \text{ cm}^{-2}$
$J$	Current density	$2.5 \text{ K.A/ cm}^{-2}$

### 2.1. The Structure of Feynman Logic gate

The proposed Feynman logic gate based on MZI-SOA is shown in Fig. 7. A structure of MZI is created of two 3db-couplers (50:50 coupler) connected by arms of equal optical length. Also two semiconductor optical amplifier (SOA) is placed into the upper and lower arms of MZI. MZI has two input ports, two output ports and the input signal is split into the two arms of the input 3db-coupler. Finally split signal, are recombined in the output combiner. In both arms, SOA used for amplification and attenuation of an optical signal.

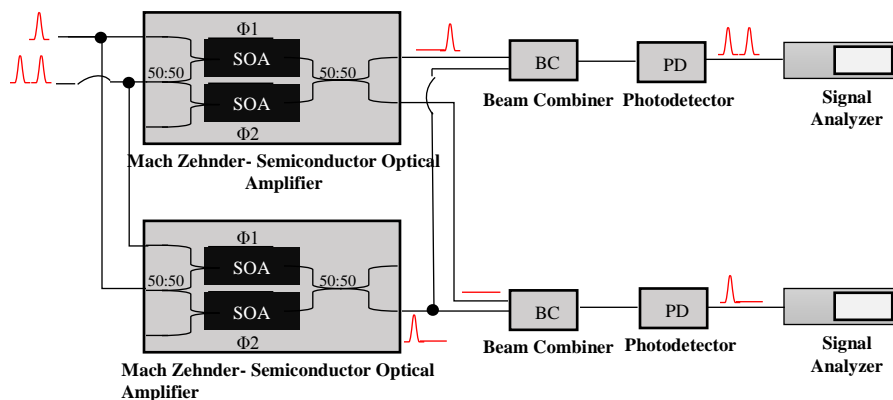


Fig. 7. The Structure of Feynman logic gate based on MZI-SOA.

With XPM effect, changing the refractive index of one of the arms, so the phase difference at the input of the 3db-combiner changed and signal switches from one output port to the other. In MZI-SOA, if one signal presented attenuated in one arm and amplified in the other arm. The working principle of the MZI-SOA can be explained as follows. In the demonstrated structure, any input signal is propagated simultaneously in the two arms of MZI. If the input signal is split at the upper coupler, more power pass through upper arm. With XPM effect in SOA, gain saturation induced and carrier density reduced, as a result, an additional  $\pi$  phase can be introduced on the upper arm because of the XPM. Now it's clear with no signal XPM effect, the input signal pass through two arms and nothing exits from the upper output port. The nonlinear switching component used was an above mentioned QD-SOA, when driven with 150mA. In this structure optical filter is placed in front of the output ports for blocking the amplified spontaneous emission (ASE) noise and Bit synchronization in the structure was achieved using optical delay.

From logic mechanism point, the proposed Feynman gate using two MZI-SOA and two beam combiner (BC) based all optical logic gate. BC is to simply combine the optical signal while the beam splitter, splits the beams into two optical signals. A Feynman gate is a 2input and 2output having the mapping (A,B) to (P=A,Q=A xor B). The demonstrated structure of Feynman gate is shown in Fig. 7.

### 3. RESULT AND DISCUSSION

We proposed a simple Feynman logic gate structure for logic application and discuss the influence of the XPM and active layer thickness on the logic operation of SOA. The QD-SOA structure was found to be optimum for the logic application. According to section 2, it is found that at a wavelength of 1.55  $\mu\text{m}$ , polarization sensitivity is smaller than 0.1 dB up to 1.7

$\mu\text{m}$  thickness and remains under 1 dB at higher thicknesses. However, the temperature rise in the active layer due to the high operating current density ( $I > 2.5\text{Ith}$ ) might be a drawback to this structure. Hence, owing to the temperature stability of the structure considering graphene material for logical application [17], [18], in future work semiconductor optical amplifier assisted with graphene plasmonic structure will be considered.

### 4. CONCLUSION

Here we have proposed the design of Feynman logic gate based on QD-SOA-MZI in telecommunication range, i.e., 1.55  $\mu\text{m}$ . The numerical result was shown that by considering the effect of both XPM and active layer thickness for propagating one polarization through the SOA, the ultrafast and low power consumption structure can be obtained. Therefore, the proposed structure can find the potential application in advanced optical devices such as optical memristors.

### REFERENCES

- [1] T. Houbavlis, K. Zoiros, M. Kalyvas, G. Theophilopoulos, C. Bintjas, K. Yiannopoulos, *et al.*, "All-optical signal processing and applications within the ESPRIT project DO/spl I. bar/ALL," *Journal of Lightwave Technology*, Vol. 23, pp. 781-801, 2005.
- [2] Y. Aikawa, S. Shimizu, and H. Uenohara, "Demonstration of all-optical divider circuit using SOA-MZI-type XOR gate and feedback loop for forward error detection," *Journal of Lightwave Technology*, Vol. 29, pp. 2259-2266, 2011.
- [3] A. Farmani and H. B. Bahar, "Hardware Implementation of 128-Bit AES Image Encryption with Low Power Techniques on FPGA to VHDL," *Majlesi Journal of Electrical Engineering*, Vol. 6, 2012.
- [4] S. H. Kim, J. H. Kim, J. W. Choi, C. W. Son, Y. T. Byun, Y. M. Jhon, *et al.*, "All-optical half adder using cross gain modulation in semiconductor optical amplifiers," *Optics Express*, Vol. 14, pp.

- 10693-10698, 2006.
- [5] J. H. Kim, Y. T. Byun, Y. M. Jhon, S. Lee, D. H. Woo, and S. H. Kim, "All-optical half adder using semiconductor optical amplifier based devices," *Optics Communications*, Vol. 218, pp. 345-349, 2003.
- [6] B. Dai, S. Shimizu, X. Wang, and N. Wada, "Simultaneous all-optical half-adder and half-subtractor based on two semiconductor optical amplifiers," *IEEE Photonics Technology Letters*, Vol. 25, pp. 91-93, 2013.
- [7] J. H. Kim, Y. M. Jhon, Y. T. Byun, S. Lee, D. H. Woo, and S. H. Kim, "All-optical XOR gate using semiconductor optical amplifiers without additional input beam," *IEEE Photonics Technology Letters*, Vol. 14, pp. 1436-1438, 2002.
- [8] J. Wang, J. Sun, Q. Sun, D. Wang, X. Zhang, D. Huang, *et al.*, "PPLN-based flexible optical logic AND gate," *IEEE Photonics Technology Letters*, Vol. 20, pp. 211-213, 2008.
- [9] J. Y. Lee, L. Yin, G. P. Agrawal, and P. M. Fauchet, "Ultrafast optical switching based on nonlinear polarization rotation in silicon waveguides," *Optics Express*, Vol. 18, pp. 11514-11523, 2010.
- [10] J. Xu, X. Zhang, and J. Mørk, "Investigation of patterning effects in ultrafast SOA-based optical switches," *IEEE Journal of Quantum Electronics*, Vol. 46, pp. 87-94, 2010.
- [11] A. Ferreira, A. Coêlho, J. Sousa, C. Sobrinho, F. Magalhães, G. Guimarães, *et al.*, "PAM-ASK optical logic gates in an optical fiber Sagnac interferometer," *Optics & Laser Technology*, Vol. 77, pp. 116-125, 2016.
- [12] A. Farmani, M. Farhang, and M. H. Sheikhi, "High performance polarization-independent Quantum Dot Semiconductor Optical Amplifier with 22dB fiber to fiber gain using Mode Propagation Tuning without additional polarization controller," *Optics & Laser Technology*, Vol. 93, pp. 127-132, 2017.
- [13] A. Kotb and K. E. Zoiros, "Performance analysis of all-optical XOR gate with photonic crystal semiconductor optical amplifier-assisted Mach-Zehnder interferometer at 160 Gb/s," *Optics Communications*, Vol. 402, pp. 511-517, 2017.
- [14] S. Al Grait and D. Maywar, "Cross-polarisation modulation-based ultrahigh contrast operation of a Fabry-Pérot all-optical AND gate," *Electronics Letters*, Vol. 52, pp. 641-643, 2016.
- [15] J. Hou, L. Chen, W. Dong, and X. Zhang, "40 Gb/s reconfigurable optical logic gates based on FWM in silicon waveguide," *Optics express*, Vol. 24, pp. 2701-2711, 2016.
- [16] M. I. Shehata and N. A. Mohammed, "Design and optimization of novel two inputs optical logic gates (NOT, AND, OR and NOR) based on single commercial TW-SOA operating at 40 Gbit/s," *Optical and Quantum Electronics*, Vol. 48, p. 336, 2016.
- [17] A. Farmani, M. Miri, and M. H. Sheikhi, "Analytical modeling of a highly tunable giant lateral shift in total reflection of light beams from a graphene containing structure," *Optics Communications*, Vol. 391, pp. 68-76, 2017.
- [18] A. Farmani, M. Miri, and M. H. Sheikhi, "Tunable resonant Goos-Hänchen and Imbert-Fedorov shifts in total reflection of terahertz beams from graphene plasmonic metasurfaces," *JOSA B*, Vol. 34, pp. 1097-1106, 2017.